



# Structural characterisation of Ru<sup>II</sup> [9]aneS<sub>3</sub> polypyridyl complexes by NMR spectroscopy and single crystal X-ray diffraction

Brian J. Goodfellow,<sup>a,c\*</sup> Victor Félix,<sup>b,c\*</sup> Sara M. D. Pacheco,<sup>c</sup>  
Júlio Pedrosa de Jesus<sup>c</sup> and Michael G. B. Drew<sup>d\*</sup>

<sup>a</sup> Departamento de Química (and Centro de Química Fina e Biotecnologia), Faculdade de Ciências e Tecnologia, Universidade Nova de Lisboa, 2825 Monte de Caparica, Portugal

<sup>b</sup> Instituto de Tecnologia Química e Biológica, Rua da Quinta Grande 6, 2780 Oeiras, Portugal

<sup>c</sup> Departamento de Química, Universidade de Aveiro, 3800 Aveiro, Portugal

<sup>d</sup> Department of Chemistry, The University, Whiteknights, Reading RG6 6AD, U.K.

(Received 24 May 1996; accepted 18 June 1996)

**Abstract**—The synthesis of a series of Ru<sup>II</sup> complexes with the thioether ligand [9]aneS<sub>3</sub> and various polypyridyl ligands was carried out using [Ru(dmso)<sub>4</sub>Cl<sub>2</sub>] as a starting material. The first synthetic step involved the introduction of the thioether ligand and the isolation of the compound [Ru([9]aneS<sub>3</sub>)(dmso)Cl<sub>2</sub>]. The polypyridyl ligands were then exchanged to give a series of complexes [Ru([9]aneS<sub>3</sub>)(X)(Cl)]<sup>+</sup> (X = 1,10-phenanthroline (phen), 2,2'-bipyridyl (bpy), 4,4'-diphenyl-2,2',-bipyridyl (dbp) and 4,7'-diphenyl-1,10-phenanthroline (dip)). These complexes were characterised by NMR and UV spectra. The complexes with X = phen and bpy were crystallised and single crystal X-ray diffraction studies carried out. Distorted octahedral coordination geometry was observed for both complexes. The equatorial planes are formed by two macrocyclic sulfur donor atoms and two nitrogen atoms from polypyridyl ligands (bpy or phen). The hexa-co-ordination is achieved *via* a chlorine and the remaining sulfur, macrocyclic atom. The [9]aneS<sub>3</sub> macrocyclic ligand adopts a [333] facial arrangement. The results from NMR studies for [Ru([9]aneS<sub>3</sub>)(phen)Cl]<sup>+</sup> and [Ru([9]aneS<sub>3</sub>)(bpy)Cl]<sup>+</sup> indicate that both complexes exist as two forms in solution with C<sub>s</sub> symmetry consistent with a [333] facial arrangement. Copyright © 1996 Elsevier Science Ltd

**Keywords:** Ru<sup>II</sup>; [9]aneS<sub>3</sub> complexes; polypyridyl ligands; crystal structures; NMR.

The interaction of ruthenium based compounds with DNA has seen much work over the last five years. Ruthenium polypyridyl complexes have been extensively studied following the work of Barton *et al.* [1] where the interaction of the two isomers of [Ru(1,10-phenanthroline)<sub>2</sub>Cl<sub>2</sub>] with B-DNA was explored. These studies [1–12] have found that there are a number of possible modes of interaction of Ru complexes with DNA, these include: intercalation, whereby the polypyridyl ligand is inserted (fully or partially) between the stacked bases of the DNA double helix, surface binding, within one of the DNA grooves, and covalent binding where ligands in the Ru complex are

replaced by heteroatoms of the DNA bases (normally the nitrogen of guanine) [2]. Spectroscopic studies have proved to be especially useful in probing the interactions between the Ru complexes and DNA.

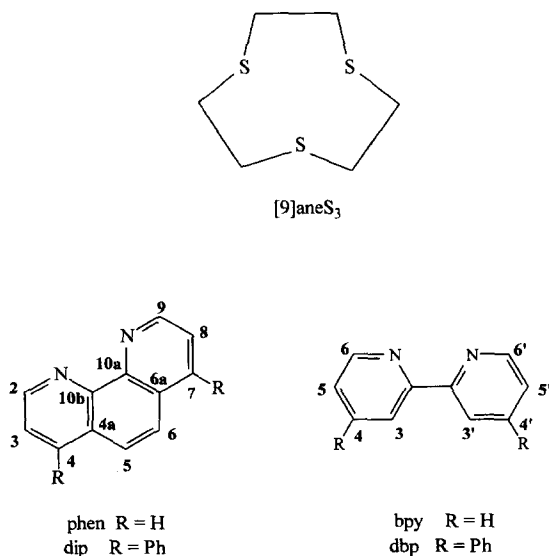
Following the work of Rosenberg *et al.* [13] in 1969 with *cis*-platin the search to find similar anti-tumor agents has been ceaseless. In the last few years, following the studies of Barton *et al.* a number of possible compounds of Ru have been discovered; Alessio *et al.* [14] found that *trans*-[Ru(dmso)<sub>4</sub>Cl<sub>2</sub>] showed promising anti-tumor activity with adjacent guanines being the preferred interaction site on DNA while Keppler *et al.* [15] Carried out an extensive study of various Ru complexes finding that [Ru(Im)<sub>2</sub>Cl<sub>4</sub>] (ImH) and [Ru(Ind)<sub>2</sub>Cl<sub>4</sub>](IndH), where Im = imidazole and Ind = indazole, show anti-tumor activity.

\* Authors to whom correspondence should be addressed.

These *in vitro* studies of Ru complexes have shown that the number and type of polypyridyl, and ancillary ligands have a profound effect on the manner and type of interaction with biomolecules. Factors such as the ability of the ligands to form H-bonds or favourable VDW interactions with the functional groups of the DNA bases have been found to play a determining role in binding. A first step in the design of Ru complexes with selective DNA binding characteristics is the choice of a suitable ligand followed by the structural characterisation of the complex.

The use of macrocyclic polyamines and polythioethers in transition metal chemistry has been considerable as these ligands are thermodynamically and kinetically inert and also have the ability to stabilise unusual oxidation states (e.g.  $\text{Rh}^{\text{II}}$ ) [16]. Krotz *et al.* [17] synthesised a series of  $\text{Rh}^{\text{III}}$  complexes with cyclic polyamines or [12]ane $\text{S}_4$  and a 9,10-diaminophenanthrene ligand in order to probe specific binding interactions to DNA. A systematic variation of thioether-polypyridyl ligands complexed to  $\text{Ru}^{\text{II}}$  would allow conclusions to be drawn as to the structural characteristics of these compounds and the role these play in DNA binding, the goal being the design of a complex with specific DNA binding characteristics. The first step in this process is, therefore, the synthesis and characterisation of the  $\text{Ru}^{\text{II}}$  based complexes followed by the determination of their three dimensional structure.

In this paper the synthesis (from  $[\text{Ru}(\text{dmsO})_4\text{Cl}_2]$ ) of a number of  $[\text{Ru}(\text{[9]aneS}_3)(\text{X})\text{Cl}]$  complexes ( $\text{X} = 1,10\text{-phenanthroline (phen), 2,2'-bipyridyl (bpy), 4,4'-diphenyl-2,2'-bipyridyl (dbp) and 4,7'-diphenyl-1,10-phenanthroline (dip)}$ ) is reported along with their spectroscopic characterisation. The structures of  $[\text{Ru}(\text{[9]aneS}_3)(1,10\text{-phenanthroline})\text{Cl}]^+$  and  $[\text{Ru}(\text{[9]aneS}_3)(2,2'\text{-bipyridyl})\text{Cl}]^+$  are compared in solution by NMR and in the solid state by X-ray crystallography.



Scheme 1.

## RESULTS AND DISCUSSION

The NMR characterisation of these complexes in solution show a number of interesting aspects. Compounds **1** and **2** seem to exist in solution in 2 forms. The  $^1\text{H}$  spectrum for the aromatic region of complex **1** is shown in Fig. 1. In a symmetric complex with  $\text{C}_{2v}$  symmetry a 1,10-phenanthroline ligand would be expected to have 4 groups of resonances from the protons at positions; 9/2, 8/3, 7/4 and 6/5 (see diagram 1). Complex **1** shows 8 groups of peaks suggesting that 2 forms exist in solution in the ratio 3:1. The peaks at 9.19(d, 5.2 Hz), 8.30(d, 8.2 Hz), 7.72(d of d, 8.4 and 5.2 Hz) and 7.62(s) ppm are from the 9/2, 7/4, 8/3 and 6/5 protons of the major form. The minor form has peaks at 9.34 (d, 5.2 Hz), 8.58(d, 8.3 Hz), 7.99(s) and 7.86(d of d, 8.2 and 5.2 Hz) ppm. The peaks from the macrocyclic ring are second order, therefore it is difficult to determine whether there are 2 sets of peaks for the thioether ligand. The  $^{13}\text{C}$  spectra for the aromatic region and the macrocyclic region for complex **1** are shown in Figs 2a and 2b. The aromatic region shows 6 sets of peaks for the major form; 152.8 (C9/C2), 146.9 (C10a/C10b), 137.2 (C7/C4), 130.2 (C4a/C6a), 127.1 and 125.5 (C8/C3 or C6/C5) ppm. The minor form has peaks at; 153.6 (C9/C2), 147.4 (C10a/C10b), 138.3 (C7/C4), 130.6 (C4a/C6a), 127.5 and 125.8 (C8/C3 or C6/C5) ppm. The  $^{13}\text{C}$  peaks of the thioether ligand also show 2 forms. The major form has peaks at 34.1, 32.1 and 31.3 ppm and the minor at 33.6, 31.6 and 31.1 ppm. Again the ratio is around 3:1. It is clear from the  $^{13}\text{C}$  data that the complex has 2 forms in solution and that the thioether ligand has 2 sets of peaks. A 2D NOESY spectrum of complex **1** was recorded to check the assignment and through space connectivities for the 2 forms. Cross peaks were observed between the thioether protons and the H-9/H-2 proton on the phenanthroline ring for both forms indicating the minor set of peaks arise from a complexed form of phenanthroline and not from the free ligand.

The NMR data for complex **2** also suggests two forms in solution. The  $^1\text{H}$  spectrum of the aromatic region for complex **2** is shown in Fig. 3. Resonances at 9.01(d, 5.6 Hz) (H-6/6'), 8.38(d, 8.1 Hz) (H-4/4'), 8.06(m) (H-5/5') and 7.56(m) (H-3/3') ppm are from the major form. The minor form has peaks at 9.11(d, 5.6 Hz), 8.47(d, 8.2 Hz), 8.17(m) and 7.66(m) ppm. The ratio between the forms is 3:1. The  $^{13}\text{C}$  spectrum of complex **2** is shown in Fig. 4. The aromatic peaks for the major form are at 156.4 (C2/2'), 152.8 (C6/6'), 138.4 (C4/4'), 127.2 (C5/5') and 123.6 (C3/3') ppm. The minor form has peaks at 156.9, 153.3, 139.3, 127.5 and 123.8 ppm. The thioether ligand for complex **2** has peaks at 34.3, 32.1 and 31.1 ppm for the major form and at 33.8, 31.7 and 31.3 ppm for the minor form.

The fact that two sets of resonances are seen for the polypyridyl and thioether ligands in complexes **1** and **2** in solution is most probably a result of the thioether

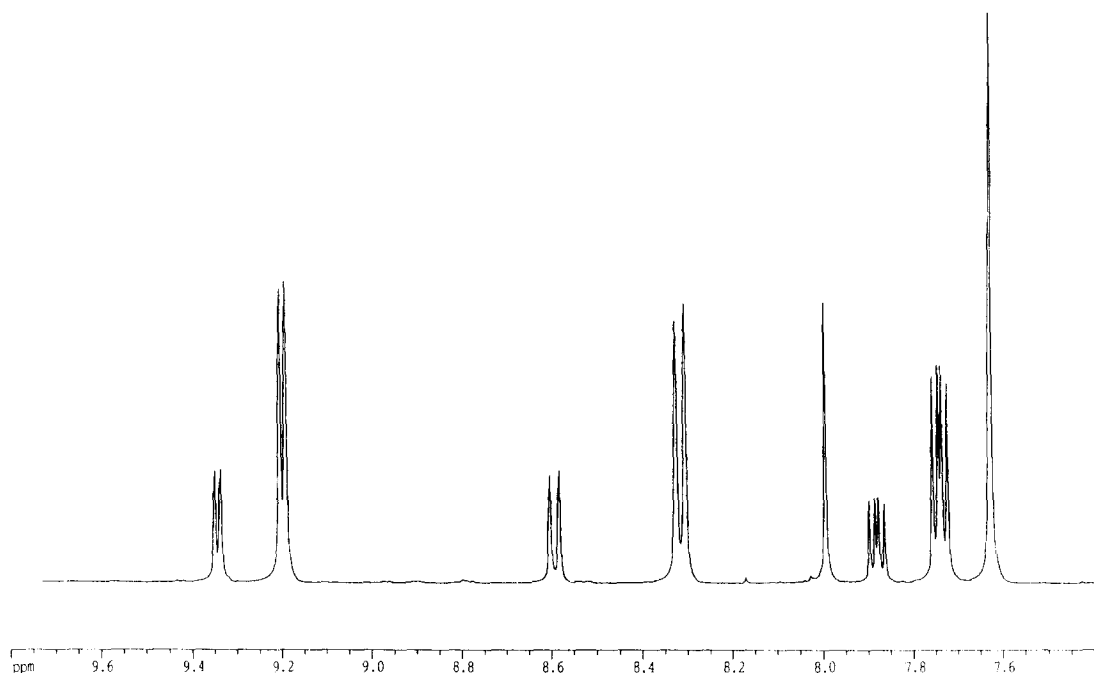


Fig. 1. The aromatic region of the  $^1\text{H}$  spectrum of complex **1** in  $\text{D}_2\text{O}$  at 303 K.

Table 1. Selected bond lengths ( $\text{\AA}$ ), angles and endocyclic torsion angles ( $^\circ$ ) for complexes **1** and **2**

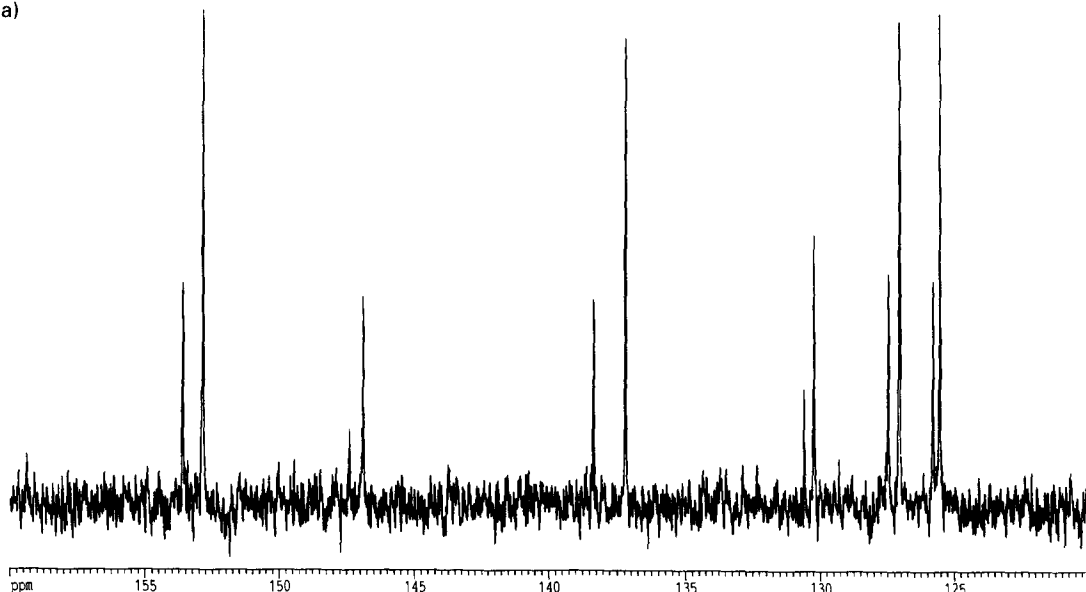
Complex	<b>1</b>	<b>2</b>
Ru(1)—N(1)	2.091(5)	2.099(6)
Ru(1)—N(2)	2.087(5)	2.112(5)
Ru(1)—S(1)	2.291(2)	2.320(2)
Ru(1)—S(2)	2.284(2)	2.316(2)
Ru(1)—S(3)	2.272(2)	2.287(2)
Ru(1)—Cl	2.438(2)	2.476(2)
N(2)—Ru(1)—N(1)	78.8(2)	78.0(2)
N(1)—Ru(1)—S(1)	174.4(1)	175.7(2)
N(2)—Ru(1)—S(1)	96.4(1)	97.8(2)
N(1)—Ru(1)—S(2)	96.8(1)	96.5(2)
N(2)—Ru(1)—S(2)	174.8(1)	174.3(2)
N(1)—Ru(1)—S(3)	94.6(1)	92.7(2)
N(2)—Ru(1)—S(3)	94.6(1)	90.2(2)
N(1)—Ru(1)—Cl	86.2(1)	88.4(2)
N(2)—Ru(1)—Cl	86.7(1)	90.2(2)
S(1)—Ru(1)—Cl	90.8(1)	90.50(8)
S(2)—Ru(1)—Cl	90.2(1)	91.24(7)
S(3)—Ru(1)—Cl	178.6(1)	178.8(1)
S(2)—Ru(1)—S(1)	87.9(1)	87.7(1)
S(3)—Ru(1)—S(1)	88.5(1)	88.4(1)
S(3)—Ru(1)—S(2)	88.5(1)	88.6(1)
S(3)—C(5)—C(6)—S(1)	-46.0(7)	-46.9(8)
C(5)—C(6)—S(1)—C(1)	135.5(5)	135.2(7)
C(6)—S(1)—C(1)—C(2)	-66.6(6)	-68.6(8)
S(1)—C(1)—C(2)—S(2)	-44.7(7)	-43.5(9)
C(1)—C(2)—S(2)—C(3)	132.1(6)	130.8(8)
C(2)—S(2)—C(3)—C(4)	-72.8(6)	70.4(7)
S(2)—C(3)—C(4)—S(3)	-41.4(8)	-45.0(9)
C(3)—C(4)—S(3)—C(5)	130.6(6)	134.1(8)
C(4)—S(3)—C(5)—C(6)	-68.9(6)	-66.1(7)

ring having 2 different conformations in solution when complexed. As only three  $^{13}\text{C}$  peaks are seen for the [9]ane $\text{S}_3$  ligand for each form (Fig. 2b) the ligand must adopt conformations where a plane of symmetry runs through the Ru, Cl and one sulfur atom and bisects the angle N—Ru—N for the polypyridyl ligand. Therefore both forms must have  $C_s$  symmetry.

The single crystal X-ray diffraction studies of complexes  $[\text{Ru}(\text{[9]aneS}_3)(\text{phen})\text{Cl}]\text{Cl}\cdot 3\text{H}_2\text{O}$  and  $[\text{Ru}(\text{[9]aneS}_3)(\text{bpy})\text{Cl}]\text{Cl}\cdot 3\text{H}_2\text{O}$  indicate hexa-coordination for the Ru centres. Molecular diagrams with corresponding atomic labelling schemes are shown in Figs 5 and 6 for cations  $[\text{Ru}(\text{[9]aneS}_3)(\text{phen})\text{Cl}]^+$  and  $[\text{Ru}(\text{[9]aneS}_3)(\text{bpy})\text{Cl}]^+$ , respectively. The selected bond lengths, angles and endocyclic torsion angles are listed in Table 1. The structural parameters associated with the Ru coordination spheres show distorted octahedral geometry for both complex cations. The equatorial planes are formed by two macrocyclic sulfur donor atoms and two nitrogen atoms from polypyridyl ligands (bpy or phen). The hexa-coordination is achieved *via* a chlorine and the remaining sulfur macrocyclic atom.

In complex **1**, the axial Ru—S bond length  $[\text{Ru—S}(3) = 2.272(2) \text{ \AA}]$  is shorter than equatorial bond lengths  $[\text{Ru—S}(1) = 2.291(2) \text{ and Ru—S}(2) = 2.284(2) \text{ \AA}]$ . A more pronounced differential *trans* influence is observed for complex **2**, where the Ru—S(3) bond length is 2.287(2) and the Ru—S(2) and Ru—S(1) bonds are 2.316(2) and 2.320(2)  $\text{\AA}$  respectively. These facts suggest that in addition to a  $\sigma$ -*trans* effect, the competitive  $\pi$  acceptance of polypyridyl ligands plays an important role in determining

(a)



(b)

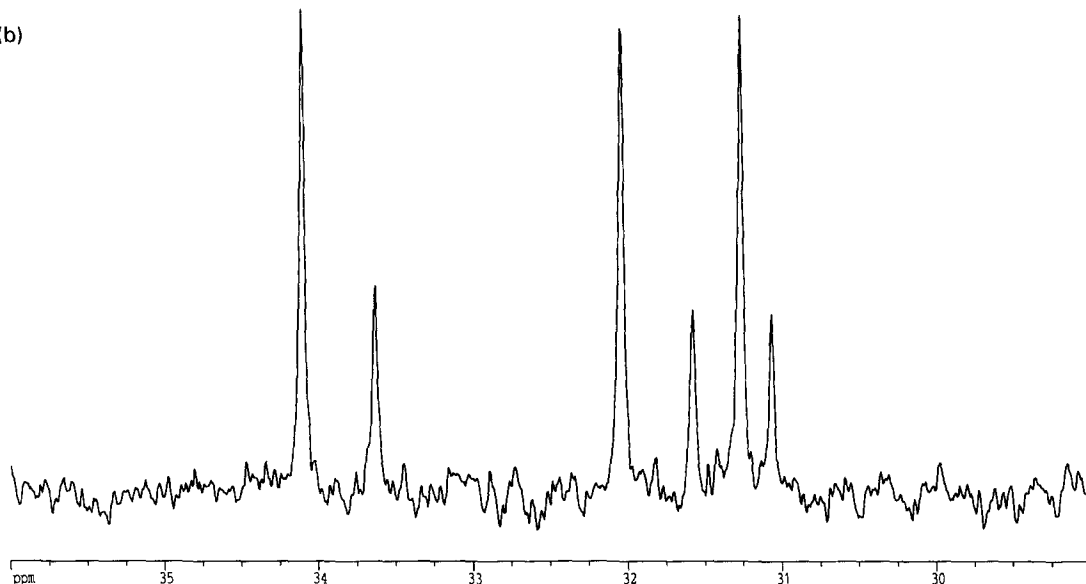


Fig. 2. (a) The aromatic region of the  $^{13}\text{C}$  spectrum in  $\text{D}_2\text{O}$  at 303 K of complex **1**. (b) The aliphatic region of the  $^{13}\text{C}$  spectrum of complex **1**.

the Ru—S bond lengths. The average bond lengths Ru—N 2.089(2) **1** and 2.106(2) **2** are similar to those observed for the octahedral complex  $[\text{Ru}(\text{NCMe})_3(\text{[9]aneS}_3)]^{2+}$  2.065(5) Å [18].

The angles in the equatorial plane involving the nitrogen atoms and metal centre differ from ideal octahedral values due to the small bite-angles of phen and bpy (78.8(2) and 78.0(2)° respectively). These values are similar to those seen for the octahedral complexes  $[\text{Ru}(\text{[12]aneS}_4)(\text{phen})]^{2+}$  79.5(4) and  $[\text{Ru}(\text{[12]aneS}_4)(\text{bpy})]^{2+}$  77.7(4) [19]. The remaining angles around the ruthenium atom in both cation complexes are very close to ideal octahedral values.

The conformation of any macrocyclic ligand can be described by a set of endocyclic torsion angles using an extended Dale nomenclature [20]. For example, the [9]aneS<sub>3</sub> macrocycle in complex cations **1** and **2** have values of the S—C—C—S, C—S—C—C and C—C—S—C torsion angles (listed in Table 1) which lead to a [333] conformation in the Dale nomenclature. This conformation has been found for many transition metal complexes characterised by X-ray diffraction where the [9]aneS<sub>3</sub> ligand adopts a facial arrangement [21]. The free [9]aneS<sub>3</sub> ligand also adopts, in the solid state, this conformation [22]. A molecular dynamics and mechanics study, in the gas

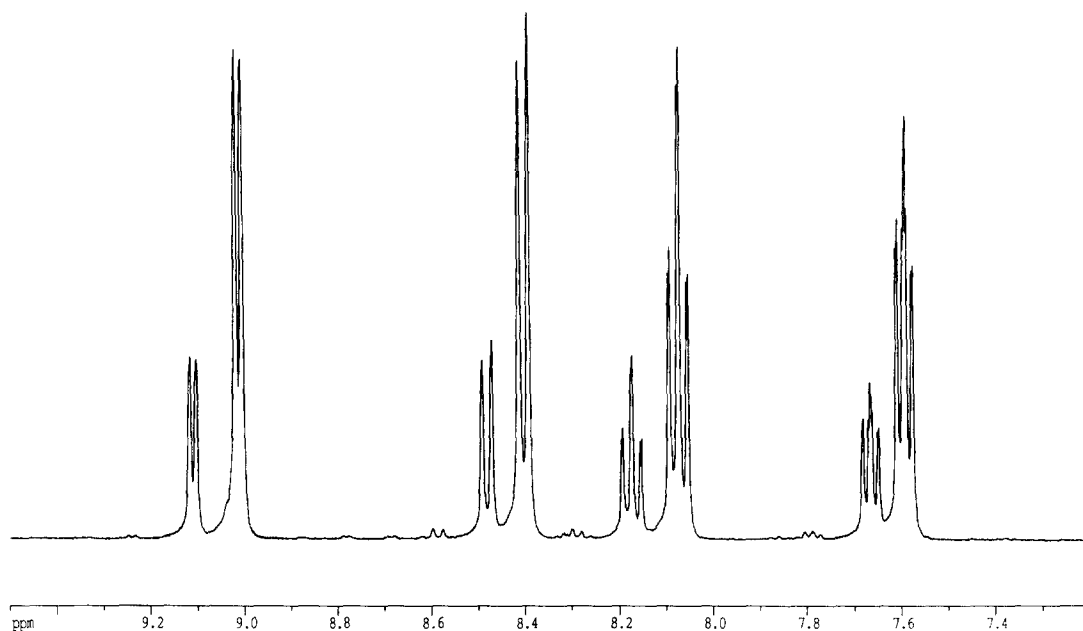


Fig. 3. The aromatic region of the  $^1\text{H}$  spectrum of complex **2** in  $\text{D}_2\text{O}$  at 303 K.

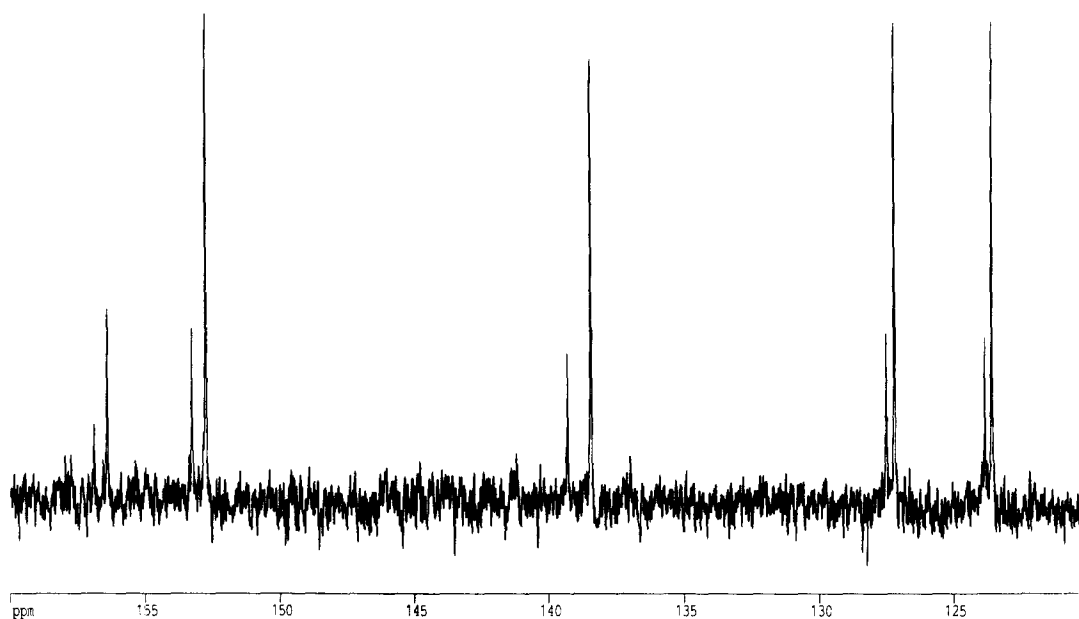


Fig. 4. The  $^{13}\text{C}$  spectrum, of the aromatic region of complex **2**.

phase [23], gave 13 conformations with energies ranging from 4.5 to 8.3 kcal/mol, the lowest energy conformation again having a [333] arrangement.

Selected intermolecular contacts are given in Table 2. In crystals of both complexes, the backbone hydrogens of the macrocyclic ligand are involved in interactions with waters of crystallization ( $\text{C}-\text{H}\cdots\text{O}$ ) and chlorine anions ( $\text{C}-\text{H}\cdots\text{Cl}$ ). The distances of these interactions are close to the sum of van der

Waals radii for H, Cl and H, O and could be considered as weak hydrogen bonds.

The results from the X-ray study are consistent with the NMR spectroscopic data for the complexes  $[\text{Ru}(\text{9})\text{aneS}_3](\text{phen})\text{Cl}]^+$  in solution, in that octahedral coordination with one thioether and one polypyridyl ligand is observed. However, the fact that the complexes **1** and **2** exist as two forms in solution and only one form is seen in the solid state suggests that

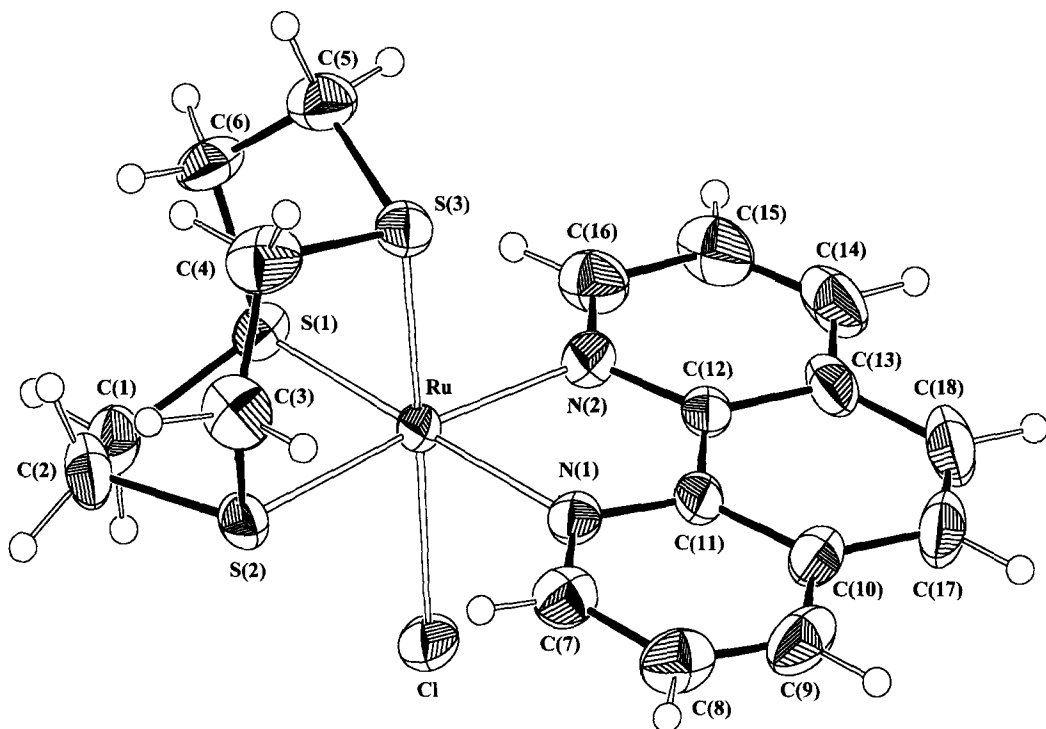


Fig. 5. Molecular structure of the  $[\text{Ru}(\text{[9]aneS}_3)(\text{phen})\text{Cl}]^+$  complex cation showing the atomic labelling scheme. Thermal ellipsoids are drawn at the 30% probability level and the hydrogen atoms are represented with a  $U_{\text{iso}}$  of  $0.01 \text{ \AA}^2$ .

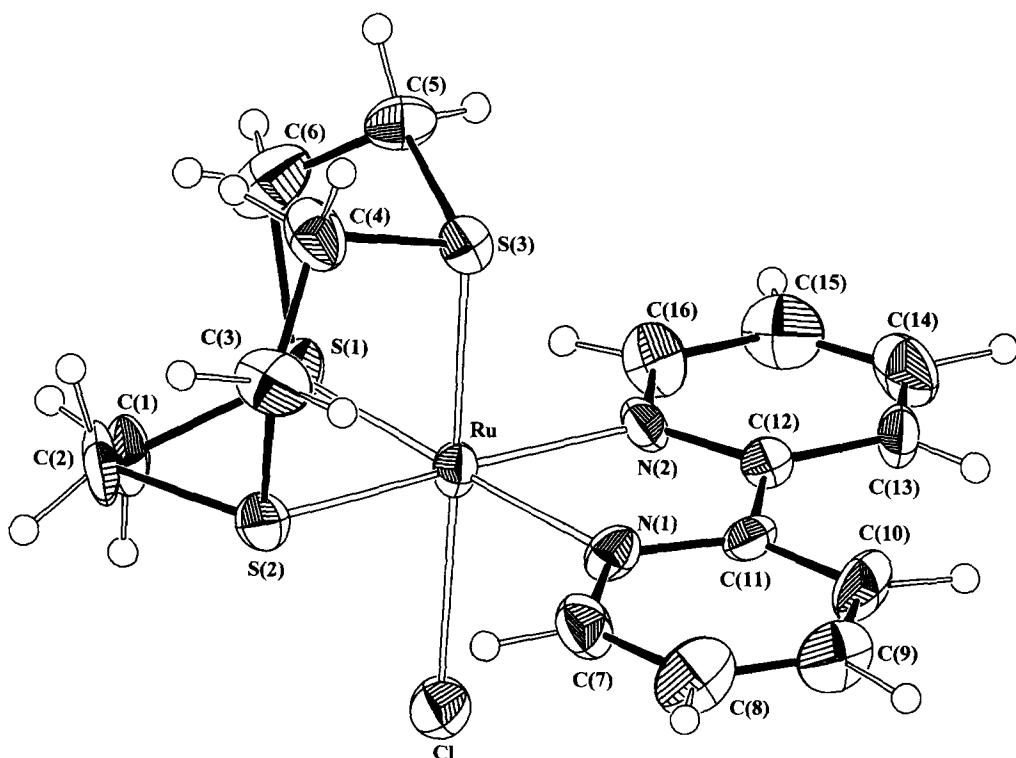


Fig. 6. Molecular structure of the  $[\text{Ru}(\text{[9]aneS}_3)(\text{bpy})\text{Cl}]^+$  complex cation showing the atomic labelling scheme. Details are as in Fig. 5.

crystal packing forces, namely the hydrogen bonds  $C-H \cdots O$  and  $C-H \cdots Cl$  stabilize the conformation adopted by the macrocycle in the solid state. These forces are absent in solution allowing the [9]aneS<sub>3</sub> ligand to adopt two different conformations (both with C<sub>3</sub> symmetry).

## EXPERIMENTAL

The ligands [9]aneS<sub>3</sub>, phen, bpy, dbp, and dip were purchased from the Aldrich Chemical Company and used without further purification.

### Syntheses

[Ru(dmsO)<sub>4</sub>Cl<sub>2</sub>]. The synthesis of [Ru(dmsO)<sub>4</sub>Cl<sub>2</sub>] was carried out according to the method of Evans *et al.* [24] NMR: <sup>1</sup>H D<sub>2</sub>O: 3.49, 3.48, 3.46, 3.43, 3.42, 3.37, 3.33 (dmsO); <sup>13</sup>C, 46.73, 46.50, 45.70, 45.11, 44.67, 44.31 (all ppm). UV/Vis: λ<sub>max</sub> nm(ε × 10<sup>-3</sup> M<sup>-1</sup> cm<sup>-1</sup>); 352(0.43), 312(0.33), 220(11.1), 202(26.9).

[Ru([9]aneS<sub>3</sub>)(dmsO)Cl<sub>2</sub>]. [Ru(dmsO)<sub>4</sub>Cl<sub>2</sub>] (0.5g, 1 mmol) was added to 0.186 g of [9]aneS<sub>3</sub> (1 mmol) in ethanol (*ca* 30 ml). The resulting suspension was refluxed for 90 min at 80 °C. A colour change from pale to bright yellow indicated reaction. The solution was concentrated and a bright yellow solid obtained. The product was washed with ethanol and dried (0.39 g, 88%). [Note: care must be taken not to use excess [9]aneS<sub>3</sub>; otherwise [Ru([9]aneS<sub>3</sub>)<sub>2</sub>]<sup>2+</sup> results.] NMR: <sup>1</sup>H D<sub>2</sub>O: 3.38s(1.5 H), 3.35s(2.4 H), 3.26s(1.5 H), (dmsO): 3.00–2.60m(12 H, [9]aneS<sub>3</sub>); <sup>13</sup>C: 43.54, 43.50, 42.12, 35.02, 34.53, 34.39, 33.50, 33.29, 31.64, 31.01, 29.21, (all ppm). UV/Vis: λ<sub>max</sub> nm(ε × 10<sup>-3</sup> M<sup>-1</sup> cm<sup>-1</sup>); 425(0.26), 352(0.40), 210(24.7).

[Ru([9]aneS<sub>3</sub>)(1,10-phenanthroline)Cl]Cl (**1**). 1,10-phenanthroline (0.48 g, 2.42 mmol, 5% excess) was added to a solution of [Ru([9]aneS<sub>3</sub>)(dmsO)Cl<sub>2</sub>] (0.1 g, 0.23 mmol) in ethanol. The yellow solution was refluxed for 15 min at 80 °C or until a colour change to orange indicated reaction had taken place. The

solution was concentrated until a yellow/orange needle or "glass wool"-like solid was obtained. On standing, large orange crystals developed. These were washed with water and dried (0.12 g, 95%). NMR: <sup>1</sup>H D<sub>2</sub>O: {9.34d, 9.19d} 2H, {8.58d, 8.30d} 2H, {7.99s, 7.62s} 2H, {7.72q, 7.86q} 2H (phen), 3.1–2.3m (12H, [9]aneS<sub>3</sub>); <sup>13</sup>C, 153.6, 152.8, 147.7, 146.9, 138.3, 137.2, 130.6, 130.2, 127.5, 127.1, 125.8, 125.5 (phen), 34.11, 33.64, 32.05, 31.58, 31.27, 31.07 ([9]aneS<sub>3</sub>). UV/Vis: λ<sub>max</sub> nm(ε × 10<sup>-3</sup> M<sup>-1</sup> cm<sup>-1</sup>); 411(3.0), 356(3.1), 297(9.6)sh, 260(22.2), 224(24.4), 200(36.0).

[Ru([9]aneS<sub>3</sub>)(2,2'-bipyridyl)Cl]Cl (**2**). A 2% excess of 2,2'-bipyridyl (0.13g, 0.858 mmol) was added to 0.250 g of [Ru([9]aneS<sub>3</sub>)(dmsO)Cl<sub>2</sub>] (0.36 g, 0.836 mmol) in ethanol. The yellow solution was refluxed for 20 min at 80 °C and an orange/red solution obtained. The solution was concentrated to dryness and redissolved in EtOH/H<sub>2</sub>O. On standing, orange/red crystals were obtained (0.42 g, 98%). NMR: <sup>1</sup>H D<sub>2</sub>O: {9.11d, 9.01d} 2H, {8.47d, 8.38d} 2H, {8.17t, 8.06t} 2H, {7.66t, 7.56t} 2H (bpy); 2.96–2.21m 12H ([9]aneS<sub>3</sub>); <sup>13</sup>C, 156.9, 156.4, 153.3, 152.8, 139.3, 138.4, 127.5, 127.2, 123.6 (phen), 34.27, 33.80, 32.09, 31.65, 31.34, 31.10 ([9]aneS<sub>3</sub>). UV/Vis: λ<sub>max</sub> nm(ε × 10<sup>-3</sup> M<sup>-1</sup> cm<sup>-1</sup>); 413(3.0), 315(4.6), 283(15.7), 241(24.1), 203(24.1).

[Ru([9]aneS<sub>3</sub>)(4,4'-diphenyl-2,2'-bipyridyl)Cl]Cl (**3**). The ligand 4,4'-diphenyl-2,2'-bipyridyl (0.062 g, 0.201 mmol) was added to a solution of [Ru([9]aneS<sub>3</sub>)(dmsO)Cl<sub>2</sub>] (0.085 g, 0.197 mmol) in ethanol. Reflux for 2 h at 80 °C gave an orange/brown solution. After concentration the brick-coloured precipitate was collected and dried (0.11 g, 84%). NMR: <sup>1</sup>H D<sub>2</sub>O: 9.07d 2H, 9.00s 2H, 8.03d 4H, 7.90d 2H, 7.60m 6H (dbp), 3.20–2.60m 12H ([9]aneS<sub>3</sub>). UV/Vis: λ<sub>max</sub> nm(ε × 10<sup>-3</sup> M<sup>-1</sup> cm<sup>-1</sup>); 422(5.4), 295(26.9), 250(21.0), 202(36.5).

[Ru([9]aneS<sub>3</sub>)(4,7'-diphenyl-1,10-phenanthroline)Cl]Cl (**4**). To the complex [Ru([9]aneS<sub>3</sub>)(dmsO)Cl<sub>2</sub>] (0.2 g, 0.464 mmol) in ethanol was added 0.157 g (0.472 mmol) of 4,7'-diphenyl-1,10-phenanthroline. After refluxing for 2 h at 80 °C a yellow

Table 2. Selected intermolecular contacts for crystal structures of the complexes **1** and **2**

Distances (Å)		Angles (°)	
<b>Complex 1</b>			
H(12) ⋯ OW(1) [−1.0 + x, y, z]	2.519	C(1)–H(12) ⋯ OW(1) [−1.0 + x, y, z]	145.0
H(52) ⋯ OW(3) [x, 1.0 + y, z]	2.485	C(5)–H(52) ⋯ OW(3) [x, 1.0 + y, z]	164.5
H(42) ⋯ Cl(1) [x, 1.0 + y, z]	2.903	C(4)–H(42) ⋯ Cl(1) [x, 1.0 + y, z]	162.7
<b>Complex 2</b>			
H(51) ⋯ OW(2) [−0.5 − x, y, 0.5 + z]	2.708	C(5)–H(51) ⋯ OW(2) [−0.5 − x, y, 0.5 + z]	150.2
H(41) ⋯ Cl(1) [−0.5 − x, y, 0.5 + z]	3.153	C(4)–H(41) ⋯ Cl(1) [−0.5 − x, y, 0.5 + z]	142.9
H(42) ⋯ Cl(1) [−x, 0.5 − y, 0.5 + z]	2.815	C(4)–H(41) ⋯ Cl(1) [−x, 0.5 − y, 0.5 + z]	150.9
H(22) ⋯ Cl(1) [−x, 0.5 − y, 0.5 + z]	2.838	C(2)–H(22) ⋯ Cl(1) [−x, 0.5 − y, 0.5 + z]	171.9
H(32) ⋯ Cl(1) [x, y, z]	2.933	C(32)–H(32) ⋯ Cl(1) [x, y, z]	160.1
H(11) ⋯ Cl(1) [0.5 − x, y, 0.5 + z]	2.848	C(32)–H(32) ⋯ Cl(1) [0.5 − x, y, 0.5 + z]	134.8

low/orange solution was obtained. Concentration of the solution yielded an orange solid (0.29 g, 91%). NMR:  $^1\text{H}$   $\text{D}_2\text{O}$ ; 9.46d 2H, 8.12s 2H, 7.88d 2H, 7.87–7.59m 10H (dip), 3.29–2.64m 12H ([9]aneS<sub>3</sub>). UV/Vis:  $\lambda_{\text{max}}$  nm( $\epsilon \times 10^{-3} \text{ M}^{-1} \text{ cm}^{-1}$ ); 386(5.2), 276(28.5), 223(24.3), 205(38.6).

#### NMR spectroscopy

All spectra were recorded in either a Bruker AMX spectrometer operating at 300 MHz or a Bruker ARX spectrometer operating at 400 MHz. The  $^1\text{H}$  spectra were obtained using 16k data points and a sweep width of 14.04 ppm. Deuterated methanol of  $\text{D}_2\text{O}$  were used as solvents with chemical shifts being referenced to HOD (4.75 ppm) or  $\text{CD}_3\text{HOD}$  (3.35 ppm).  $^{13}\text{C}$  spectra were recorded using a sweep width of 250 ppm with 32k data points. Full proton decoupling was used. External dioxan (66.5 ppm) was used as a chemical shift reference. The 2D NOESY [25] spectrum (800 ms mixing time) was recorded at 400 MHz. A sweep width of 14.04 ppm and a recycle delay of 10 s was used. The number of  $t_1$  increments was 512 with 8 scans being co-added for each increment. The number of data points used was 2048. The final matrix size was  $2\text{K} \times 2\text{K}$  with a q sine window applied in both dimensions.

#### Crystallographic measurements and processing

The pertinent crystal data and refinement details for complexes **1** and **2** are given in Table 3. Single crystal data for complex **1** were collected with an Enraf-Nonius CAD-4 diffractometer, using a graphite-monochromated Mo- $K_\alpha$  radiation ( $\lambda = 0.71069 \text{ \AA}$ ). The unit cell parameters were calculated by least-squares refinement of 25 well centred reflections within the range  $10 < \theta < 15^\circ$ . The intensity data were collected by  $\omega$ - $2\theta$  scan mode. Three strong reflections were measured every 3600 s and their intensities did not show appreciable decay. The data were corrected for absorption and polarization effects with CAD-4 software.

Data for complex **2** were collected with a MAR-research image plate system, using a graphite-monochromated Mo- $K_\alpha$  radiation ( $\lambda = 0.71069 \text{ \AA}$ ). Single crystal was positioned at 75 mm from the plate. An exposure time of 2 min was used per  $2^\circ$  frame collected. Data analysis was carried out with XDS program [26]. Intensities were not corrected for absorption effects.

#### Structure analysis and refinement

The positions of the ruthenium atoms were obtained from three-dimensional Patterson maps and

Table 3. Crystal data and details of refinement of complexes **1** and **2**

	1	2
Formula	$\text{C}_{18}\text{H}_{26}\text{Cl}_2\text{N}_2\text{O}_3\text{RuS}_3$	$\text{C}_{16}\text{H}_{22}\text{Cl}_2\text{N}_2\text{O}_3\text{RuS}_3$
<i>M</i>	586.6	558.5
Crystal system	Monoclinic	Orthorhombic
Space group	$P2_1/n$	$Pbca$
<i>a</i> (Å)	11.753(2)	10.354(7)
<i>b</i> (Å)	8.047(6)	33.062(22)
<i>c</i> (Å)	23.952(4)	13.125(7)
$\beta$ (°)	101.83(8)	(90)
<i>V</i> (Å <sup>3</sup> )	2217.2(6)	4493.0
<i>Z</i>	4	8
<i>D<sub>c</sub></i> (g cm <sup>-3</sup> )	1.758	1.651
$\mu$ (Mo- $K_\alpha$ ) (cm <sup>-1</sup> )	1.255	1.233
<i>F</i> (000)	1192	2256
Instrument	CAD-4 Four Circle Diffractometer	MAR-research Image Plate System
$2\theta_{\text{max}}$ (°)	50	50
Index ranges	$0 \leq h \leq 13, -2 \leq k \leq 9, -28 \leq l \leq 27$	$0 \leq h \leq 8, -38 \leq k \leq 38, -9 \leq l \leq 12$
Measured reflections	5657	5425
Unique reflections ( <i>R<sub>m</sub></i> )	3893 (0.0399)	2134 (0.0533)
Data-to-parameters ratio	3885/268	2134/272
Goodness-of-fit on <i>F</i> <sup>2</sup>	0.914	0.869
Final <i>R<sub>1</sub></i> and <i>wR<sub>2</sub></i> values [ <i>I</i> > 2σ( <i>I</i> )]	0.0412; 0.1031	0.0439, 0.1235
(all data)	0.0620, 0.1391	0.0564, 0.1361
Parameters <i>a</i> , <i>b</i> in weighting scheme <sup>a</sup>	0.0709, 11.69	0.1005, 31.74
Largest difference peak and hole (e Å <sup>-3</sup> )	0.978, -0.558	0.645, -0.839

<sup>a</sup> $w = 1/[\sigma^2(F_o^2) + (aP)^2 + bP]$ ,  $P = [\text{Max}(F_o^2) + 2F_o^2]/3$ .

the remaining non-hydrogen atom positions by successive difference Fourier synthesis. The methylenic hydrogens were included in the refinement in calculated positions for idealized tetrahedral geometry while the aromatic hydrogens were found from difference Fourier maps. The hydrogen atoms of water molecules in both complexes were not found in final Fourier maps and were not included in the refinement. The hydrogens were refined with global isotropic thermal parameters. Anisotropic temperature factors were used for all non-hydrogen atoms. The structures were refined by least squares methods until convergence was achieved. The final refinements were made on  $F^2$  using a weighting system, with the form  $w = 1/[\sigma^2(F_o^2) + (aP)^2 + bP]$ ,  $P = [\text{Max}(F_o^2) + 2F_c^2]/3$  (see Table 3).

All calculations required to solve and refine the structures were carried out with SHELXS86 [27] and SHELX93 [28]. The atomic scattering factors were taken from [29]. The molecular diagrams were drawn with ORTEP II [30].

Additional material is available from the Cambridge Crystallographic Data Centre and comprises atomic coordinates, thermal parameters and the remaining bond lengths and angles.

*Acknowledgements*—We thank the E.P.S.R.C and the University of Reading for the image plate system and Insituto Superior Técnico for the CAD-4 diffractometer. We also thank Mr A. W. Johans for his technical assistance with crystallographic investigations. V. F. acknowledges the Junta Nacional de Investigaçao and British Council for a travel grant.

## REFERENCES

- J. K. Barton and E. Lolis, *J. Am. Chem. Soc.* 1985, **107**, 708.
- C. V. Kumar, J. K. Barton and N. J. Turro, *J. Am. Chem. Soc.* 1985, **107**, 5518.
- J. K. Barton, *Science* 1986, **233**, 727.
- J. K. Barton, J. M. Goldberg, C. V. Kumar and N. J. Turro, *J. Am. Chem. Soc.* 1986, **108**, 2081.
- A. M. Pyle, J. P. Rehmman, C. V. Kumar, N. J. Turro and J. K. Barton, *J. Am. Chem. Soc.* 1989, **111**, 3051.
- A. M. Pyle and J. K. Barton, *Prog. Inorg. Chem: Bioinorg. Chem.* 1990, **38**, 413.
- C. Hiort, B. Norden and A. Rodger, *J. Am. Chem. Soc.* 1990, **112**, 1971.
- J. P. Rehmman and J. K. Barton, *Biochem.* 1990, **29**, 1710.
- M. Eriksson, M. Leijon, C. Hiort, B. Nordem and A. Graslund, *J. Am. Chem. Soc.* 1992, **114**, 4933.
- S. S. David and J. K. Barton, *J. Am. Chem. Soc.* 1993, **115**, 2984.
- S. A. Tysoe, R. J. Morgan, A. D. Baker and T. C. Streckas, *J. Phys. Chem.* 1993, **97**, 1707.
- K. Naing, M. Takahashi, M. Taniguchi and A. Yamagishi, *Inorg. Chem.* 1995, **34**, 350.
- B. Rosenberg, L. VanCamp, J. E. Trosko and V. Mansour, *Nature* 1969, **222**, 385.
- E. Alessio, G. Mestroni, G. Nardin, W. M. Attia, M. Calligaris, G. Sava and S. Zoret, *Inorg. Chem.* 1988, **27**, 4099.
- B. K. Keppler, M. Henn, U. M. Juhl, M. R. Berger, R. Niebl and F. E. Wagner, *Prog. Clinical Biochem.* 1989, **10**, 41.
- S. R. Cooper, S. C. Rawle, R. Yagbasan and D. J. Watkin, *J. Am. Chem. Soc.* 1991, **113**, 1600.
- A. H. Krotz, L. Y. Kuo and J. K. Barton, *Inorg. Chem.* 1993, **32**, 5963.
- C. Landgrafe and W. S. Sheldrick, *J. Chem. Soc., Dalton Trans.* 1994, 1885.
- B. J. Goodfellow, S. M. D. Pacheco, J. Pedrosa de Jesus, M. G. B. Drew and Vitor Félix (unpublished results).
- J.C. A. Boeyens and S. M. Dobson, *Stereochemical and Stereophysical Behavior of Macrocycles* (Edited by I. Bernal) Vol. 2. 1. Elsevier, Amsterdam (1987).
- Cambridge Crystallographic Data Base, update (1996).
- R. S. Glass, G. S. Wilson and W. N. Setzer, *J. Am. Chem. Soc.* 1980, **102**, 1068.
- J. Beech, P. J. Cragg and M. G. B. Drew, *J. Chem. Soc., Dalton Trans.* 1994, 719.
- I. P. Evans, A. Spencer and G. Wilkinson, *J. Chem. Soc., Dalton Trans.* 1973, 204.
- S. Macura and R. R. Ernst, *Mol. Phys.* 1980, **41**, 95.
- W. Kabsch, *J. Appl. Crystallogr.* 1988, **21**, 916.
- G. M. Sheldrick, *SHELXS-86*, in *Crystallographic Computing 3*, (Edited by G. M. Sheldrick, C. Krüger and R. Goddard). Oxford University Press (1985).
- G. M. Sheldrick, *SHELX-93, Program for Crystal Structure Refinement*, University of Göttingen (1994).
- International Tables for X-Ray Crystallography*, Vol. 4, Kynoch Press, Birmingham (1974).
- C. K. Johnson, ORTEP II, A Fortran Thermal-ellipsoid, Plot Program, for Crystal Structure Illustrations. Report ORNL-5138, Oak Ridge National Laboratory, Oak Ridge, TN (1976).